

Collisional Decoherence Observed in Matter Wave Interferometry

Klaus Hornberger, Stefan Uttenthaler, Björn Brezger, Lucia Hackermüller, Markus Arndt, and Anton Zeilinger*

Universität Wien, Institut für Experimentalphysik, Boltzmanngasse 5, A-1090 Wien, Austria

(Dated: March 14, 2003)

We study the loss of spatial coherence in the extended wave function of fullerenes due to collisions with background gases. From the gradual suppression of quantum interference with increasing gas pressure we are able to support quantitatively both the predictions of decoherence theory and our picture of the interaction process. We thus explore the practical limits of matter wave interferometry at finite gas pressures and estimate the required experimental vacuum conditions for interferometry with even larger objects.

PACS numbers: 03.75.-b, 03.65.Yz, 39.20.+q

Matter wave interferometers are based on *quantum* superpositions of spatially separated states of a single particle. However, as is well known, the concept of wave-particle duality does not apply to a *classical* object which by definition never occupies macroscopically distinct states simultaneously. By performing interference experiments with particles of increasing complexity one can therefore probe the borderline between these incompatible descriptions.

It is still a matter of debate how to explain the quantum-to-classical transition in a unified framework. Some theories contain an element beyond the unitary evolution of quantum mechanics [1, 2] — which includes the ‘collapse’ of the wave function as taught in many standard textbooks. Decoherence theory, on the other hand, remains within the framework of the quantum theory [3, 4, 5]. It explains the decay of quantum coherences as being caused by the interaction of the quantum object with its environment.

So far, several decoherence experiments in atom interferometry focused on the loss of coherence due to scattering of a single [6, 7] or a few [8] laser photons by an atom. Other authors proposed or realized schemes to encode which-path information in internal atomic degrees of freedom, thereby reducing the interference contrast as well, in spite of a negligible change in the atomic center-of-mass state [9, 10]. These studies are complemented by experiments which quantitatively followed the decoherence of a coherent photon state in a high-finesse microwave cavity [11] or of the motional state of a trapped ion [12]. However, all these experiments worked with few-level systems and engineered environments.

In the present letter we quantitatively investigate a mechanism which seems to be among the most natural and most effective sources of decoherence in our macroscopic world, namely collisions with gas particles. From the controlled suppression of quantum interference as a function of the gas pressure we are able to test both the predictions of decoherence theory and our picture of the collisional interaction.

We note that the effect of atomic collisions in an atom interferometer was already investigated in [13]. How-

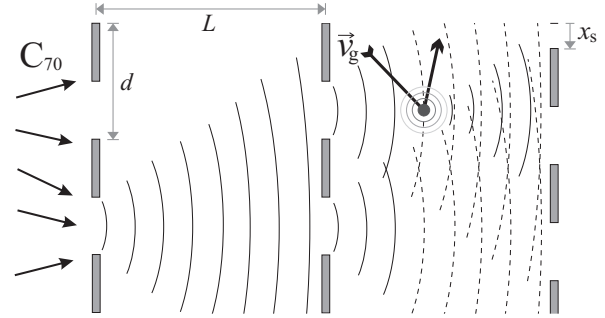


FIG. 1: Schematic setup of the near-field interferometer for C_{70} fullerenes. The third grating uncovers the interference pattern by yielding an oscillatory transmission with lateral shift x_s . Collisions with gas molecules localize the molecular center-of-mass wave function leading to a reduced visibility of the interference pattern.

ever, decoherence effects were not observed in these experiments, since the *detected* atoms did not change the state of the colliding gas sufficiently to leave behind the required path information for decoherence. In contrast to that, our experiment uses *massive* C_{70} -fullerene molecules, and is based on a Talbot-Lau interferometer (TLI) with a *wide* acceptance angle. Consequently, a fullerene molecule still enters the detector after a typical collision, while the gas particle is left in a state distinguishing the path taken.

Recently, the theoretically optimal interference contrast could be observed in our high-vacuum TLI [14], in spite of the high mass, temperature and complexity of the fullerenes. This permits us to study now the gradual loss of interference with increasing background gas pressure. The central part of the experiment is sketched in Fig. 1. An uncollimated, thermal beam of C_{70} fullerenes passes three identical vertical gold gratings, with a grating period of $d=991$ nm and a slit width of 475 nm. They are separated by an equal distance of $L = 0.22$ m which is the Talbot length $L_\lambda \equiv d^2/\lambda$ for molecules with a velocity of 106 m/s (corresponding to a de Broglie wave length of $\lambda = 4.46$ pm). A horizontal laser beam behind the third grating ionizes the molecules regardless of their

horizontal position. Three height constrictions — the oven orifice, the laser beam, and a horizontal slit halfway between — determine the parabolic trajectories in the gravitational field and thus select a narrow velocity distribution ($\Delta v/v = 8\%$) out of the molecular beam.

The TLI is based on a near-field interference phenomenon, the Talbot-Lau effect. For a specific molecular wave length it generates a high-contrast density pattern at the position of the third grating, which is an image of the second one. The quantum interferogram is then recorded by counting the number of laser ionized fullerenes as a function of the lateral position of the third grating x_s . Quantum mechanics predicts a transmission periodic in x_s with period d (see Fig. 2),

$$T(x_s) = \sum_{\ell \in \mathbb{Z}} T_\ell \exp\left(2\pi i \ell \frac{x_s}{d}\right). \quad (1)$$

The Fourier coefficients T_ℓ depend strongly on the molecular de Broglie wavelength λ (for $\ell \neq 0$) as given in [15]. They are determined by the grating configuration and include the attractive Casimir-Polder interaction between the fullerenes and the gold gratings. From the observed λ -dependence of the high-vacuum fringe visibility we find that the signal is certainly caused by near-field quantum interference, and not by classical dynamics [14, 15].

In the following we use the TLI as a means of monitoring the evolution of an extended, partially coherent quantum state of the molecular center-of-mass. The interaction with gas particles is examined by filling the vacuum chamber with various gases at low pressure ($p \leq 2.5 \times 10^{-6}$ mbar) and room temperature.

In order to relate the expected loss of interference to decoherence theory [3, 4, 16, 17] we define the *decoherence function* η as a factor to the density matrix of the molecular center-of-mass state $\rho_0(\mathbf{r}, \mathbf{r}')$. It describes the loss of coherence, i.e, the reduction of the off-diagonal elements in position representation, after one scattering event,

$$\rho(\mathbf{r}, \mathbf{r}') = \rho_0(\mathbf{r}, \mathbf{r}') \eta(|\mathbf{r} - \mathbf{r}'|). \quad (2)$$

This form follows from a trace over the scattered gas particle. It implies that the mass of the incident particle is much smaller than the fullerene mass and that the distribution of the incoming velocities is isotropic.

The reduction of interference is obtained by evolving the molecular state from the first to the third grating subject to (2) which is equivalent to solving the corresponding master equation in paraxial approximation. While a detailed derivation will be given elsewhere, it is sufficient to note that the final effect of collisional decoherence is described completely by a modification of the Fourier coefficients,

$$T_\ell \rightarrow T_\ell \exp\left(-2n\sigma_{\text{eff}} \int_0^L \left[1 - \eta\left(\ell \frac{z\lambda}{d}\right)\right] dz\right). \quad (3)$$

Here, n is the density of the gas environment and σ_{eff} the effective total cross section which accounts also for the thermal velocity distribution $g(v_g)$ in the gas. We note that the component T_0 is left unchanged by (3), since $\eta(0) = 1$ as required from the conservation of probability in (2). It follows that the average transmission remains constant, i.e, the equation describes the decoherence induced by the gas, but no losses.

In order to obtain a kinematic interpretation of (3) we first discuss the specific form of the decoherence function η for large molecular masses. By extending the analysis in [3, 5, 16] and assuming an isotropic interaction potential, described by the scattering amplitude f , we find

$$\eta(\Delta r) = \int_0^\infty dv_g \frac{g(v_g)}{\sigma(v_g)} \int d\Omega |f(\cos(\theta))|^2 \times \text{sinc}\left(\sin\left(\frac{\theta}{2}\right) \frac{2m_g v_g \Delta r}{\hbar}\right). \quad (4)$$

Here, the second integral covers the scattering angles of the gas particle. For $\Delta r = |\mathbf{r} - \mathbf{r}'| \rightarrow 0$ it yields the total cross section $\sigma(v_g)$ and we retrieve $\eta(0) = 1$. At finite separations Δr the sinc function reduces the contributions of the scattering amplitude as the deflection angle θ grows, i.e. with an increasing momentum transfer during the collision. The relevant length scale is set by the reciprocal momentum transfer in units of \hbar .

Compare this to the coherence in the molecular state which is needed to contribute to the ℓ th Fourier component of the signal. In order to illuminate coherently a region of size d/ℓ on the third grating from a distance z the required correlation in momentum must have a scale δp with $\delta p/p \times z \simeq d/\ell$. Hence, $2\pi\hbar/\delta p \simeq \ell z\lambda/d$ which motivates the form of (3): Whenever the momentum kick experienced by the molecule at a distance z is large enough to destroy the required correlations the molecule will not contribute to the interference signal. The integration in (3) covers all scattering positions between the second and the third grating, and by symmetry also those between the first and the second one (yielding the factor 2).

The case of weak decoherence, where a single event yields only partial which-way information, was studied in [6, 7, 8]. There the spatial coherence in the center-of-mass state had a smaller scale than the resolution set by the average momentum kick. The present experiment explores the opposite regime since the relevant path separations $\Delta r = \ell z\lambda/d$ are by orders of magnitude larger than the average reciprocal momentum kick for almost all z . It follows that the relevant long range coherences are destroyed completely and independently of the separation Δr . This simplifies the integration in (3) since we can now set $\eta = 0$ for $\ell \neq 0$ implying a localization rate which is determined only by the effective cross section. Since the fringe contrast of our experiment is essentially determined by the basic Fourier component T_1 [15] we

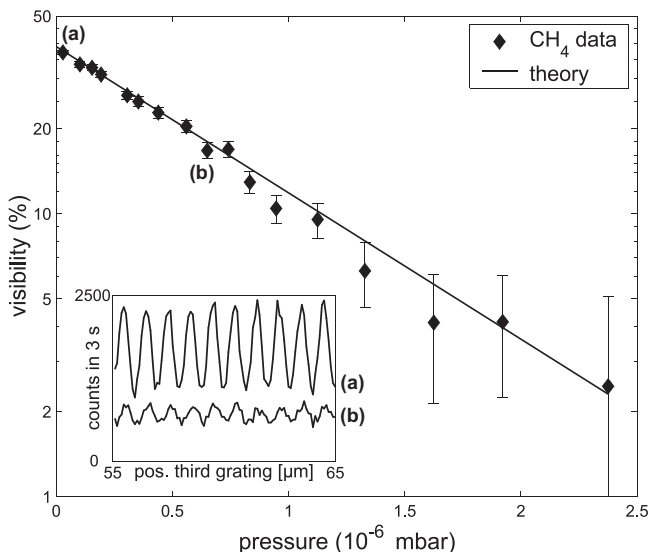


FIG. 2: Fullerene fringe visibility vs. methane gas pressure on a semi-logarithmic scale. The exponential decay indicates that each collision leads to a complete loss of coherence. The solid line gives the prediction of decoherence theory, see text. The inset shows the observed interference pattern at (a) $p = 0.05 \times 10^{-6}$ mbar and (b) $p = 0.6 \times 10^{-6}$ mbar.

thus expect a visibility of

$$V(p) = 2 \frac{|T_1|}{T_0} \exp\left(-\frac{2L\sigma_{\text{eff}}}{k_B T} p\right) =: V_0 e^{-p/p_0} \quad (5)$$

as a function of the gas pressure $p = nk_B T$. Note that although simple collisional loss may lead to an exponential drop in count rate, loss alone will not affect the visibility. The exponential decay of the fringe contrast described by (5) is a genuine effect of decoherence.

An experimental demonstration of collisional localization is presented in Fig. 2. It shows the pressure dependence of the fringe visibility in the presence of methane gas. A central molecular velocity of $v_m = 117$ m/s was chosen, corresponding to a maximal vacuum visibility of 41% [14]. The quantitative agreement with our model (the solid line in Fig. 2) is obtained by extending the above reasoning by two additional points.

First, the momentum transfer is *not* isotropic in our experiment due to the directed motion of the molecules. Nonetheless, any collision localizes the molecule, and the conclusion remains valid that the loss of coherence in (3) is determined only by σ_{eff} . However, in the effective cross section the velocities of both the molecule v_m and the gas must be taken into account. Since the collisions are governed by the isotropic London dispersion force [18, 19] they are determined by a single parameter C_6 (see Tab. I). Following [18] and after an integration over the thermal distribution $g(v_g)$ we find

$$\sigma_{\text{eff}}(v_m) = \frac{C_6^{2/5}}{\hbar^{2/5}} \frac{\tilde{v}_g^{3/5}}{v_m} \left(8.4946 + 1.6989 \frac{v_m^2}{\tilde{v}_g^2} \right) \quad (6)$$

gas	C_6	gas	C_6	gas	C_6
H ₂	0.80	CH ₄	3.3	Ar	2.3
D ₂	0.77	N ₂	2.1	Kr	3.4
He	0.31	Ne	0.71	Xe	5.1

TABLE I: Van der Waals parameters for the interaction of C₇₀ fullerenes with various gases, in units of meV nm⁶ (obtained as outlined in [19] using data from [20]).

with \tilde{v}_g the most probable velocity in the gas. This expression, which is an asymptotic expansion for small v_m/\tilde{v}_g , predicts an effective cross section which exceeds the geometric one by *two* orders of magnitude.

The second point to be considered are the corrections due to the particular constraints in our experiment, notably the gravitational velocity selection and the finite size of the detector. On the one hand, even those collisions which occur outside of the interferometer can change the visibility since they alter the direction of the molecule in the uncollimated beam, which reshuffles the observed velocity classes as a function of the gas pressure. On the other hand, due to the finite width of the detector, the observed molecules from the selected velocity class suffered on average less collisions than the undetected ones. In order to account for these effects we solve the *classical* phase space dynamics using a Monte Carlo method. Our predictions for the visibility are then obtained by weighting Eq. (5) with the classical velocity distribution of those molecules which reach the detector.

As seen from Fig. 2 our calculation, which contains no adjustable parameters, agrees well with the observed decrease of the visibility. The simulation also reproduces the pressure dependence of the count rates and of the measured velocity distributions.

The loss of coherence with increasing pressure is de-

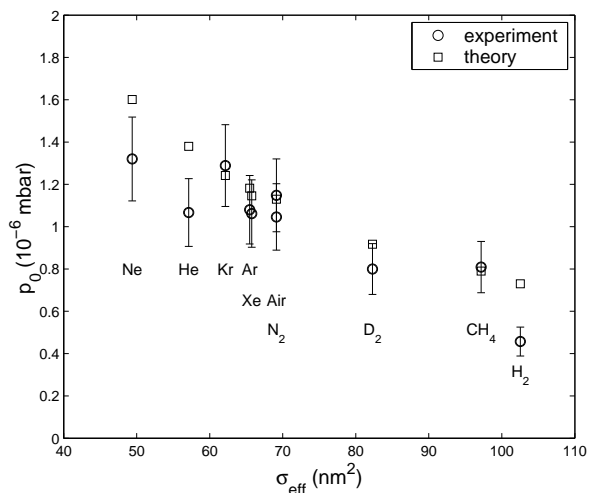


FIG. 3: Experimental decoherence pressure p_0 for various gases compared to the predictions of decoherence theory.

scribed by the “decoherence pressure” p_0 defined in (5). It is determined experimentally by an exponential fit to the pressure dependent visibilities as in Fig. 2. Figure 3 compares the measured values of p_0 to the theoretical predictions for a number of mono-atomic and molecular gases [23]. We find a very satisfactory agreement over the whole broad range of masses and interaction strengths – both of which cover almost two orders of magnitude. The experimental error is mainly due to the uncertainty in the pressure measurement (about 15%). The uncertainty of the theoretical values amounts to about 5% (not drawn in the figure) and is related to lacking information about the velocity dependence of the fullerene detection efficiency.

Most remarkable in Fig. 3 is the weak dependence of the decoherence pressure on the specific type of collision partners. This can be explained if we assume that the polarizability and therefore also C_6 are proportional to the mass of the scattered particle m_g . Then (6) shows that the mass dependencies of the interaction constant and of the mean gas velocity almost cancel out leaving $\sigma_{\text{eff}} \propto m_g^{1/10}$. This remaining dependence is so weak that the deviations in the interaction constants due to the particular electronic structure of the gases outweigh the bulk behavior. Xenon, for example, as the heaviest gas used, lies right in the middle of the observed range of decoherence pressures. We also note that the effect of molecular background gases does not deviate systematically from atomic ones.

Finally, based on the good overall agreement between experiment and theory we can estimate the vacuum conditions that are required for the successful observation of quantum interference of much larger objects. For the sake of an appealing example, let us consider a virus with a mass of $M = 5 \times 10^7$ amu interacting with molecular nitrogen (air) at room temperature. Since the static polarizability of large hydrocarbons is closely proportional to their mass the Slater-Kirkwood approximation [21, Chap. 13.3] for the van der Waals parameter yields $C_6(M-N_2)/\text{meVnm}^6 \simeq 3.5 \times 10^{-3} M/\text{amu}$. Equations (5) and (6) then predict a decoherence pressure of $p_0/\text{mbar} \simeq 2.7 \times 10^{-11} \text{ sec } v_m/L$. By inserting $L = 1$ m for the interferometer size and $v_m = 10$ m/s for the velocity we find that collisions would not limit quantum interference in a TL-interferometer even for an object as large as a virus, provided we can reduce the background pressure to below $p \simeq 3 \times 10^{-10}$ mbar. This is certainly feasible with available techniques.

In conclusion, our experiments investigate for the first time the effect of decoherence due to collisions with various gases. They are in very good quantitative agreement with decoherence theory. While we are currently investigating other possible limits of matter wave interferometry – such as the emission of blackbody radiation – it seems safe to rephrase a famous word by R. Feynman [22]: There is plenty of room at the *top*.

This work has been supported by the European TMR

network (No. HPRN-CT-2000-00125), the FWF projects F1505 and START Y177. BB has been supported by an EU Marie Curie fellowship (No. HPMF-CT-2000-00797), and KH by the DFG Emmy Noether program.

* www.quantum.univie.ac.at

- [1] G. C. Ghirardi, A. Rimini, and T. Weber, Phys. Rev. D **34**, 470 (1986).
- [2] R. Penrose, Gen. Rel. Grav. **28**, 581 (1996).
- [3] E. Joos and H. D. Zeh, Z. Phys. B. **59**, 223 (1985).
- [4] W. H. Zurek, Phys. Today **44**, 36 (1991).
- [5] M. Tegmark, Found. Phys. Lett. **6**, 571 (1993).
- [6] T. Pfau, S. Spälter, C. Kurtsiefer, C. Ekstrom, and J. Mlynek, Phys. Rev. Lett. **73**, 1223 (1994).
- [7] M. S. Chapman, T. D. Hammond, A. Lenef, J. Schmiedmayer, R. A. Rubenstein, E. Smith, and D. E. Pritchard, Phys. Rev. Lett. **75**, 3783 (1995).
- [8] D. A. Kokerowski, A. D. Cronin, T. D. Roberts, and D. E. Pritchard, Phys. Rev. Lett. **86**, 2191 (2001).
- [9] M. Scully, B.-G. Englert, and H. Walther, Nature **351**, 111 (1991).
- [10] S. Dürr, T. Nonn, and G. Rempe, PRL **81**, 5705 (1998).
- [11] M. Brune, E. Hagley, J. Dreyer, X. Maître, A. Maali, C. Wunderlich, J. M. Raimond, and S. Haroche, Phys. Rev. Lett. **77**, 4887 (1996).
- [12] C. J. Myatt, B. E. King, Q. A. Turchette, C. A. Sackett, D. Kielpinski, W. M. Itano, C. Monroe, and D. J. Wineland, Nature **403**, 269 (2000).
- [13] J. Schmiedmayer, M. Chapman, C. Ekstrom, T. Hammond, S. Wehinger, and D. Pritchard, Phys. Rev. Lett. **74**, 1043 (1995).
- [14] B. Brezger, L. Hacker Müller, S. Uttenthaler, J. Petschinka, M. Arndt, and A. Zeilinger, Phys. Rev. Lett. **88**, 100404 (2002).
- [15] B. Brezger, M. Arndt, and A. Zeilinger, J. Opt. B, (2003), in press.
- [16] M. R. Gallis and G. N. Fleming, Phys. Rev. A **42**, 38 (1990).
- [17] T. P. Altenmüller, R. Müller, and A. Schenzle, Phys. Rev. A **56**, 2959 (1997).
- [18] G. C. Maitland, M. Rigby, E. B. Smith, and W. A. Wakeham, *Intermolecular Forces - Their Origin and Determination* (Clarendon Press, Oxford, 1981).
- [19] A. Ruiz, J. Bretón, and J. M. Gomez Llorente, Chem. Phys. Lett. **270**, 121 (1997).
- [20] H. A. Jiménez-Vázquez and R. J. Cross, J. Chem. Phys. **104**, 5589 (1996); D. Yin and A. D. MacKerell, J. Comp. Chem. **19**, 334 (1998); S. Maruyama and T. Kimura, Proc. ASME Heat Transfer Division **2**, 405 (2000).
- [21] J. O. Hirschfelder, C. F. Curtiss, and R. B. Bird, *Molecular Theory of Gases and Liquids* (John Wiley & Sons, New York, 1954).
- [22] R. Feynman (1959), APS meeting, Caltech, Pasadena, see <http://www.zyvex.com/nanotech/feynman.html>.
- [23] The high-vacuum visibility did not reach its optimal value in all of our measurements, although it stayed significantly above the classical value. We checked that the observed p_0 was independent of the attainable maximum visibility, which is consistent with attributing the visibility loss to vibrational noise.